TRANSACTIONS OF THE INSTITUTE OF FLUID-FLOW MACHINERY

No. 135, 2017, 87–100

Mirosław Łuniewski and Jacek Pozorski*

Spatial distribution and settling velocity of heavy particles in synthetic turbulent fields**

Institute of Fluid-Flow Machinery, Polish Academy of Sciences, Fiszera 14, 80-231 Gdańsk, Poland

Abstract

We analyse numerically the motion of small inertial particles, subject to gravity, in two simple velocity fields: two-dimensional cellular flow, and a three-dimensional flow being the superposition of random Fourier velocity modes. The latter, also known as the kinematic simulation or synthetic turbulence, has often been applied in various studies, including those aiming to predict particle dispersion. The interplay of the particle inertia and the acceleration of gravity has non-trivial consequences for trajectories of particles and their spatial distribution, known as a preferential concentration. Also, we compute the average settling velocity of particles in function of their inertia and the number of fluid velocity modes used in simulations. The present paper aims to study these efects, as the synthetic turbulence represents an interesting option for subfilter modeling in particle-laden large-eddy simulation.

Keywords: Two-phase flow; Heavy particles; Turbulent dispersion

1 Introduction

Particle-laden turbulent flows are common in environmental studies and industrial applications, such as cyclone separators, pulverised coal burners or steam turbines. Actually, the inertial particle motion and separation from a flow was the first research topic of one of the authors, undertaken with the late Professor Romuald

*Corresponding author. E-mail address: jp@imp.gda.pl

** Dedicated to the memory of professor Romuald Puzyrewski (1935–2016)

Puzyrewski. We calculated then the droplet separation efficiency from the wet steam flow in the last turbine stages [15]. Years later, that study naturally further evolved to inquiry about the effects of turbulence on particle motion and wall deposition, see [12] for introduction.

Nowadays, the large-eddy simulations (LES) become increasingly often used for modelling of turbulent flows as a powerful alternative to statistical closures, see [1], also for two-phase systems with the dispersed particles or droplets. Since the small-scale structures are smoothed out (by definition of LES, [11]), the question appears whether, when, and how the impact of those structures on the dispersed particles or droplets should be modelled. This point, called the subfilter or subgrid particle modelling, has received a lot of attention in the literature for the last 20 years or so, yet there is no ultimate answer so far. We have studied the issue in wall-bounded turbulence, see [5, 14] and references therein, and recently also in isotropic turbulence laden with particles subject to gravity [17]. The effect of subfilter scales on one-particle dispersion in free turbulence has been relatively well addressed, less so the impact on two-point or relative dispersion, on particle collisions, or break-up of agglomerates. The presence of gravity adds to the difficulty of the problem. In wall-bounded flows, a suitable subgrid particle modelling for wall deposition or resuspension remains another open issue. It appears that for some of the phenomena, structural subgrid particle closures are needed. In other words, we look for approaches where the subgrid fluid velocity field is reconstructed or mimicked in a possibly computationally inexpensive way. One of the options is to use analytically prescribed fields that are kinematically correct (divergence-free in incompressible cases), yet their dynamics is not reconstructed. Among them are the cellular flow and the so-called cheap turbulence model, or kinematic simulations (KS). Both flow fields have been studied long time ago in the context of particle dispersion and settling velocity [7, 8], but only recently KS have been proposed as subfilter models for particles in LES [4, 18].

The main aim of the work reported here has been to scrutinise such velocity fields, known as "synthetic turbulence", and to have some hands-on experience with using them. In the next term, these possible candidates for structural subfilter closures will be assessed in particle-laden LES.

2 Basic formulae

The analysis of the particle motion begins with determining the fluid velocity field, in which the particles will move under the influence of gravity.

First, we consider the two-dimensional cellular velocity field [8], described by

$$u_x = U_0 \sin(x/L) \cos(z/L) , \quad (1)$$

$$u_z = -U_0 \cos(x/L) \sin(z/L) , \quad (2)$$

where u_x nad u_z are the horizontal and vertical components of velocity, respectively, L is the characteristic length scale and U_0 is the fluid velocity scale. The cellular field (CF) is steady and periodic by construction; it is illustrated in Fig. 1(a).

A second velocity field to be studied here is constructed as the superposition of N random, Fourier velocity modes [2]:

$$\mathbf{u}(\mathbf{x}) = \sum_{n=1}^{N} \left[\mathbf{u}_1(\mathbf{k}_n) \cos(\mathbf{k}_n \cdot \mathbf{x}) + \mathbf{u}_2(\mathbf{k}_n) \sin(\mathbf{k}_n \cdot \mathbf{x}) \right] , \quad (3)$$

where $\mathbf{k}_n$ is the wavenumber vector, $\mathbf{x}$ is the position vector. The random vectors $\mathbf{u}_1$ and $\mathbf{u}_2$ are constructed as the cross products, $\mathbf{u}_1(\mathbf{k}_n) = \boldsymbol{\zeta}_n \times \mathbf{k}_n$ and $\mathbf{u}_2(\mathbf{k}_n) = \boldsymbol{\xi}_n \times \mathbf{k}_n$, to satisfy the continuity equation of incompressible fluid:

$$\mathbf{k}_n \cdot \mathbf{u}_1(\mathbf{k}_n) = \mathbf{k}_n \cdot \mathbf{u}_2(\mathbf{k}_n) = 0 \quad \Longrightarrow \quad \mathrm{div}\mathbf{u} = 0. \quad (4)$$

Components of the vectors $\boldsymbol{\zeta}_n$ and $\boldsymbol{\xi}_n$ are chosen randomly from the standard Gaussian distribution. The components of the wavenumber vector $\mathbf{k}_n$ are chosen randomly from the uniform distribution over a sphere. Figure 1(b) shows velocity vectors in a realisation of the resulting KS field in the x-z plane (for $N = 16$ random modes) whereas Fig. 2 shows the isocontours of the horizontal velocity component in KS for two values of N.

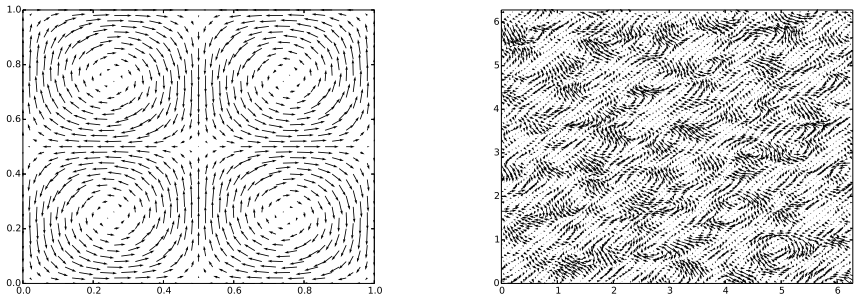

(a) (b)

Figure 1: Velocity vectors of: (a) cellular flow field, (b) KS with $N = 16$ modes.

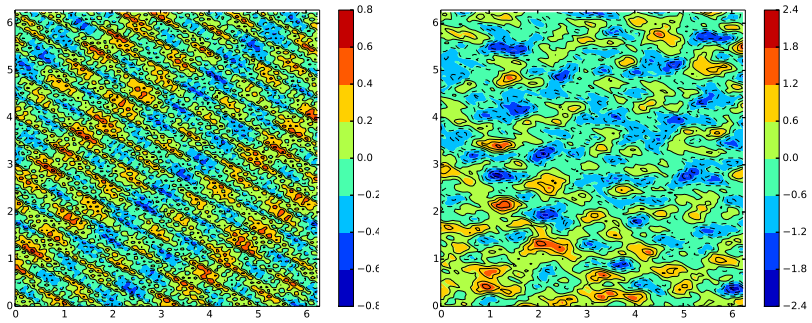

(a) (b)

Figure 2: Contours of the synthetic velocity field, horizontal component: (a) $N = 8$, (b) $N = 32$. N is the number of Fourier modes in KS.

The equations describing the dynamics of the particles are in the form

$$\frac{d\mathbf{x}_p}{dt} = \mathbf{v}_p \,, \tag{5}$$

$$\frac{d\mathbf{v}_p}{dt} = \frac{1}{\tau_p}(\mathbf{u} - \mathbf{v}_p) + \mathbf{g} \,, \tag{6}$$

where $\mathbf{u} = \mathbf{u}(\mathbf{x}_p)$ is the fluid velocity at the particle location, $\mathbf{v}_p$ is the particle velocity and $\mathbf{g} = g\mathbf{z}_0$ is gravitational acceleration. A system of N_p particles will be considered, yet the current particle index is skipped in Eqs. (5)–(6) and in the following for simplicity. The product of the particle relaxation time, τ_p, and the gravitational acceleration determines the particle settling velocity (in the fluid at rest), called the terminal velocity:

$$V_T = \tau_p g \,. \tag{7}$$

The behaviour of particles suspended in a fluid flow is characterised by two dimensionless quantities. The first one is the non-dimensional time scale, or the Stokes number, defined as

$$\mathrm{St} = \frac{\tau_p U_0}{L}, \tag{8}$$

where the particle relaxation time is $0.01 \leq \tau_p \leq 1$. It is a characteristic time required for a particle to adjust its velocity to a new condition of forces in the fluid. The range of the Stokes numbers considered in the simulations is shown in Tab. 1. Another non-dimensional quantity governing the particle motion is the

non-dimensional velocity scale, introduced as the ratio of V_T and U_0 for cellular flow.

Table 1: The Stokes numbers.

Characteristic fluid velocity U_0	Min value ($\tau_p = 0.01$)	Max value ($\tau_p = 1$)
0.1	0.002	0.2
0.2	0.004	0.4
0.3	0.006	0.6
0.4	0.008	0.8
0.5	0.01	1.0
0.6	0.012	1.2
0.7	0.014	1.4
0.8	0.016	1.6
0.9	0.018	1.8
1.0	0.02	2.0

The system of Eqs. (5)–(6) was integrated using the exponential implicit scheme. For horizontal components, here u_x, and the vertical one, u_z, it is written as

$$v_{p,x}^{n+1} = v_{p,x}^{n} \exp\left(-\Delta t/\tau_p\right) + u_x^{n+1}\left[1 - \exp\left(-\Delta t/\tau_p\right)\right] , \tag{9}$$

$$v_{p,z}^{n+1} = v_{p,z}^{n} \exp\left(-\Delta t/\tau_p\right) + \left(u_z^{n+1} - \tau_p g\right)\left[1 - \exp\left(-\Delta t/\tau_p\right)\right] , \tag{10}$$

where $t^{n+1} = t^n + \Delta t$ and Δt is the time step. Such formulae are useful for small inertia particles since otherwise the stability criterion of the standard explicit schemes, $\Delta t < \tau_p$, may result in prohibitively small time steps of the simulation. For the integration of particle positions, a simple explicit scheme has been applied

$$\mathbf{x}_p^{n+1} = \mathbf{x}_p^n + \mathbf{v}_p^n \Delta t \, . \tag{11}$$

This scheme is not fully consistent with Eqs. (9)–(10), yet for sufficiently small time steps it converges with the more complex formulae that result from the exact integration of Eqs. (9)–(10) over a time step Δt.

3 Particle trajectories and distribution in space

For the case of cellular flow (CF) field, the particles were regularly arranged (at equal intervals) on the horizontal section of length $2L$, in the middle of the first cell ($z = 0.25$). For the case of kinematic simulations (KS), the particles were arranged at equal intervals on the length $2L$ at $z = 0.5L$, where $L = 2\pi/|\mathbf{k}_1|$. In both CF and KS cases, it is assumed that the particle initial velocity equals 0.

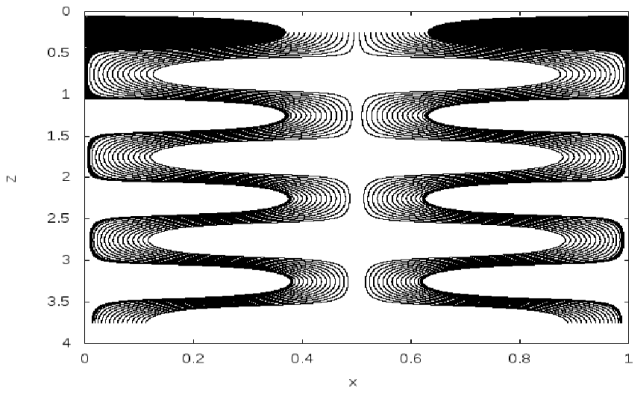

(a) St = 0.006

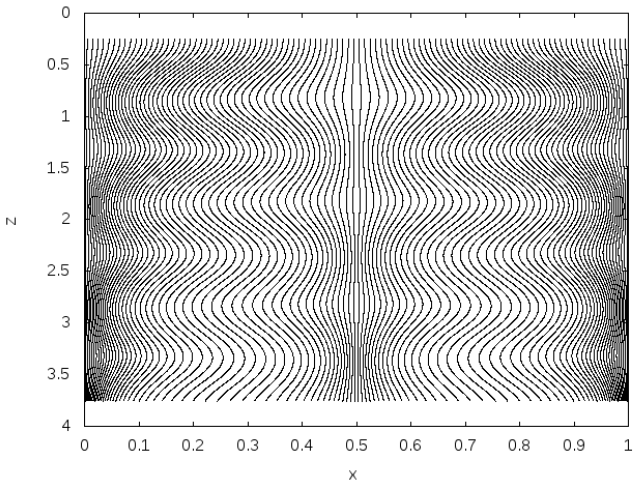

(b) St = 0.06

Figure 3: Particles trajectories in cellular flow ($U_0 = 0.3, L = 0.5$).

Examples of computed particle trajectories in the cellular flow are shown in Figure 3. With the increase in the Stokes number, the particle trajectories flatten, i.e.

they become less sensitive to the structure of the flow field. In Fig. 3(a) are shown the elliptical-helical trajectories of the particles of St = 0.006 in the initial phase of their movement. The picture is further magnified in Fig. 4(a). This effect of particle capture within a vortical structure occurs for particles whose terminal velocity, V_T, is less than the amplitude of the fluid velocity, U_0. The number of captured particles increases with increasing difference between these two parameters $\Delta V = U_0 - V_T$ (see Fig. 4). A number of the exact trajectories of selected particles are shown in Fig. 5. The differences of the trajectories result from the initial locations of the particles.

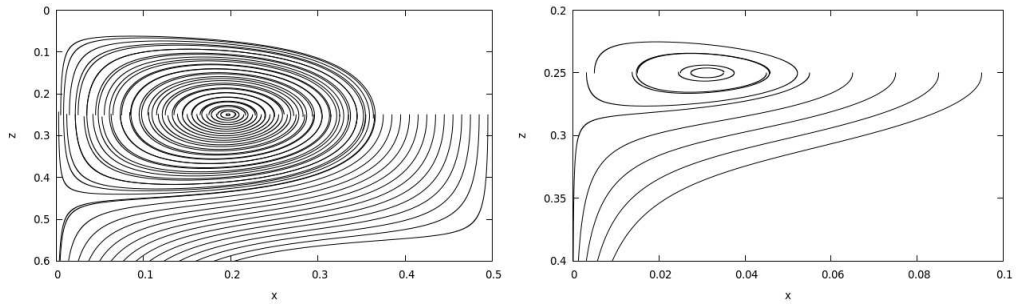

(a) $\Delta V \approx 0.2$ (St = 0.006) (b) $\Delta V \approx 0.006$ (St = 0.018)

Figure 4: Examples of the eliptical particle trajectories in CF ($\Delta V = U_0 - V_T$), single rotation cycle ($N_p = 35$ and $N_p = 5$ particles respectively).

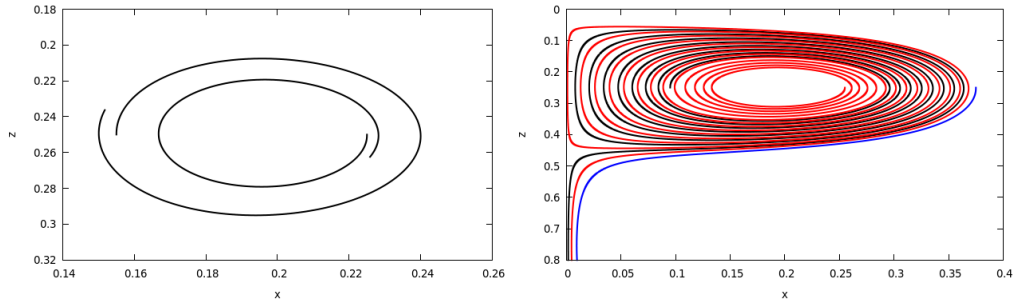

(a) (b)

Figure 5: Trajectories of selected particles in CF: (a) first rotation depending on the starting point, St = 0.006; (b) three different trajectories, St = 0.018.

Examples of particle trajectories from kinematic simulations are shown in Figs. 6,

7, and 8. With the increase of the particle relaxation time, the trajectories flatten. If the velocity field is 'periodic', the particles trajectories are 'periodic' too. With a larger number of the included Fourier modes, the flattening of trajectory occurs at a larger particle relaxation time. Particle trajectories without gravity were first analysed in [3] to assess a flow mode which can be identified with turbulent dispersion in KS.

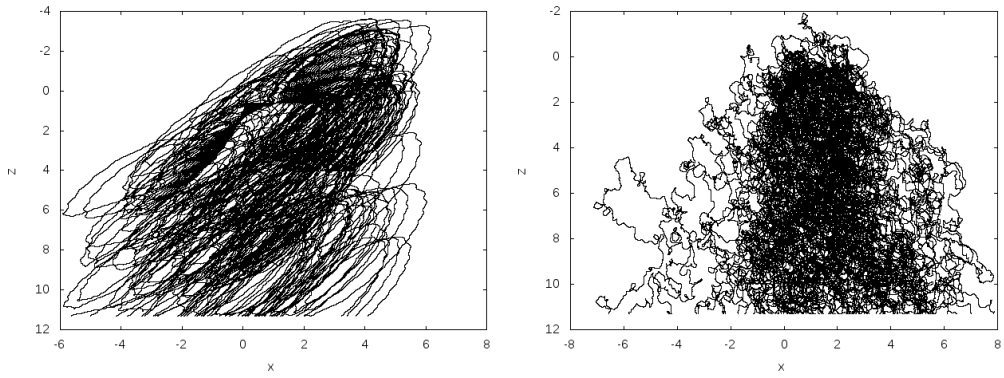

(a) $N = 4$ (b) $N = 8$

Figure 6: Particles trajectories in KS at $\tau_p = 0.01$; simulations with a different number of velocity modes N.

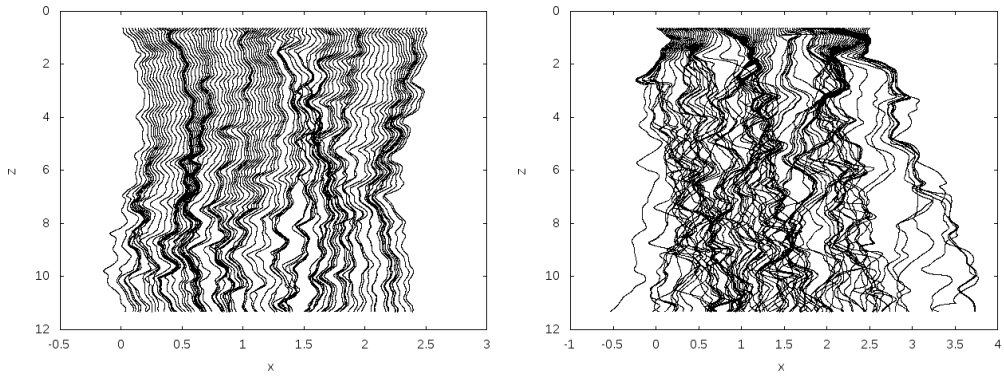

(a) $N = 8$ (b) $N = 16$

Figure 7: Particle trajectories in KS at $\tau_p = 0.1$; simulations with a different number of velocity modes N.

The particle trajectories are readily represented in plots for 2D flow cases. Yet, in general (including for 3D flows), it is quite informative to analyse the statistics

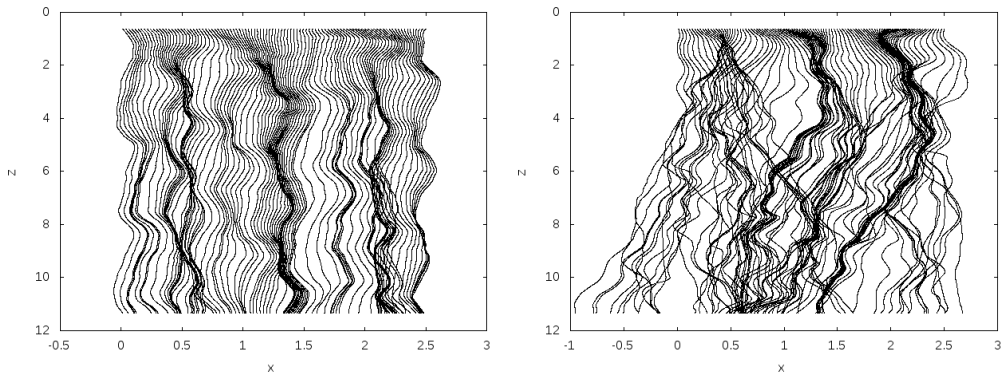

(a) $N = 16$ (b) $N = 32$

Figure 8: Particle trajectories in KS at $\tau_p = 0.2$; simulations with a different number of velocity modes N.

of particle locations in space. The non-uniformity of particle distribution, due to their interaction with the underlying flow structures, is called the preferential concentration or the clustering phenomenon. It is readily observed in experiments [9] and in fully resolved numerical simulations of turbulent flows [6]. There are various measures of preferential concentration [10]. Previously, we have applied the techniques of bin counting and the computation of the radial distribution function [13]. In the present work, we have used the method of Voronoi tesselation, first proposed for particle-laden flows in [9]. In thin 2D horizontal slices of the computational domain, we have constructed the Voronoi cells (polygons) out of the particle locations, $p = 1, 2, \ldots, N_p$, at a given time instant, accounting for the periodicity of the particle distribution in each slice. The number of equidistant slices was 20 to obtain reasonable statistics and the particle locations were considered independent in each slice. In Fig. 9, a typical Voronoi tesselation is shown, corresponding to the locations of two classes of inertial particles in KS at a final time of simulation. The particle distribution in space is statistically steady, the clustering effects are visible.

Then, a good quantitative measure of preferential concentration is provided through the Voronoi histograms. Let A_p be the area of the Voronoi cell containg particle p. A suitably normalised histogram becomes the probability density function (PDF), denoted as $f_A(a)$, of the area normalised by the mean value, $a = A/\langle A \rangle$. The PDF is further compared with the one corresponding to the uniform, random distribution of particles in space, described by the Poisson distribution whose standard deviation is $\sigma_A = 0.52$. When the preferential concentration

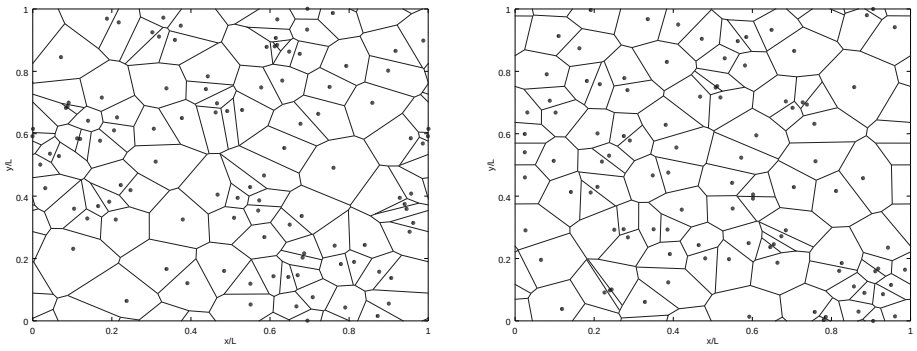

(a) (b)

Figure 9: The Voronoi tesselation applied to the statistically-steady distribution of inertial particles in KS; a horizontal slice of the flow domain. Particles of: (a) $\tau_p = 0.01$, (b) $\tau_p = 0.1$. Particle locations are indicated by $\bullet$.

of particles is present, then the values of σ_A and also the PDF tails at small and large A (corresponding to particle clusters and voids, respectively) are higher than those for the uniform distribution. The histograms of the normalised Voronoi area for heavy particles in KS are shown in Fig. 10. At the initial time, the standard deviation of the cell area PDF is very close to that corresponding to the random distribution; at a final time, it becomes somewhat larger ($\sigma_A = 0.56$) indicating the presence of preferential concentration (see also symbols in the figure).

It is interesting to note that a nice visualisation, resembling typical preferential concentration patterns in a flow laden with small particles, is presented on the front cover of a successful textbook on fluid mechanics, co-authored by the late professor Puzyrewski [16].

4 Average settling velocity of the particles

The statistical samples for each choice of parameters (St and U_0) consisted of 100 particles. In the case of cellular flow, due to the large variability of particle trajectories, the start times of collecting information about the particles were determined in two ways. The particles whose characteristic time was less than $\tau_p = 0.3$ were counted after reaching the distance of $5L$. Larger particles were counted after reaching the time of $5\tau_p$. The selection of such running start points provides a stable period of the particle trajectories. The determination of the average speed of particles was carried on the section $2L$. Figure 11 shows the

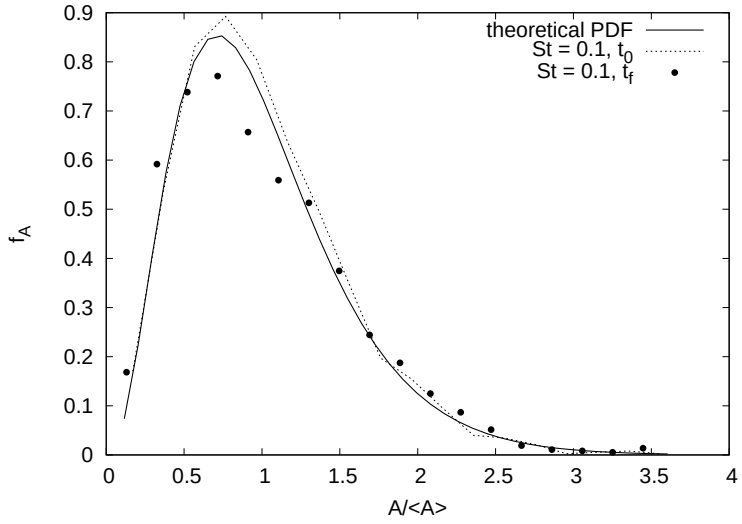

Figure 10: The PDF of the normalised area of Voronoi cells constructed for $\tau_p = 0.1$ particles in KS out of horizontal slices in the flow domain. The theoretical PDF corresponding to a random uniform distribution in 2D (solid line), the computed PDF corresponding to the initial (dotted line), and final (•) particle distribution.

influence of the velocity scale U_0 on the settling velocity of the particles in CF. In terms of the value of U_0 exceeding the velocity V_T (see Fig. 11(a)), the averaged vertical component z of the particle velocity significantly exceeds the terminal velocity V_T. This illustrates the monotonic increase in the value for the smallest St number (see Fig. 11(b)). When the two velocities V_T and U_0 become close to each other, the minimum moves to the right with the Stokes number.

In the case of KS, the start time of collecting particle information was chosen after reaching the distance of $3L$. The selection of such running start points provides a stable period of the particle trajectories. The determination of the average velocity of particles was carried on the section $6L$ with further averaging over 10 flow realisations.

For more complex velocity fields ($N = 16$ and 32), the averaged component z of the particle velocity exceeds the value of the fall velocity V_T (see also [19]). This is illustrated by the monotonic increase of the value for the smallest V_T considered (Fig. 12). The maximum value of the difference between averaged velocity $\langle V_z \rangle$ and terminal velocity V_T increases with the number of the Fourier modes and it corresponds to a larger value of the falling velocity.

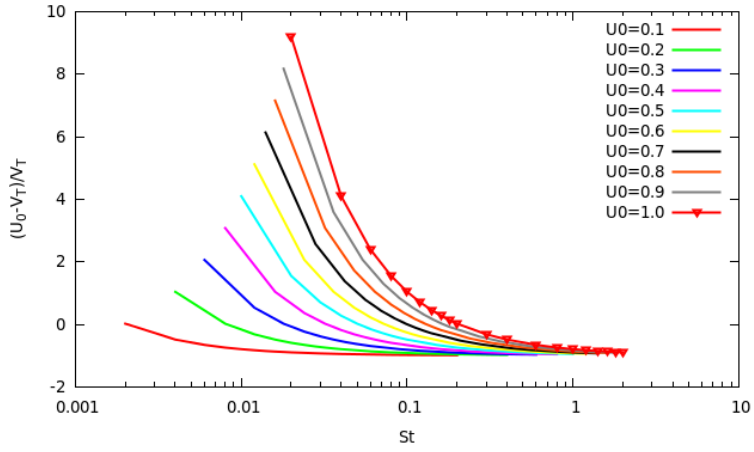

(a)

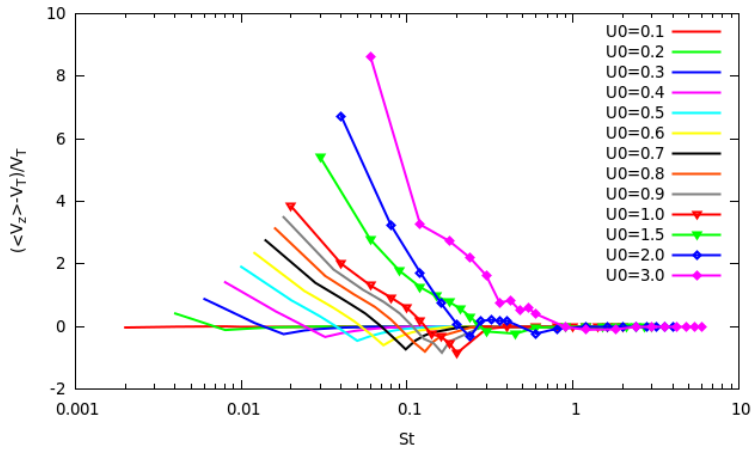

(b)

Figure 11: The average settling velocity of particles in CF, normalised with the terminal velocity V_T: (a) amplitude of the fluid velocity, (b) averaged vertical component of the particle velocity $\langle V_z \rangle$.

5 Conclusion

In the paper, we have considered a simple, two-dimensional cellular velocity field and the kinematic simulations with a number of spatial modes of different wave

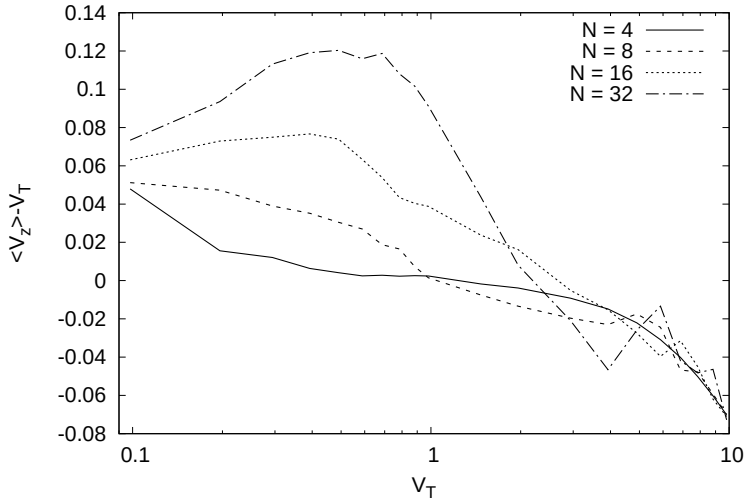

Figure 12: Kinematic simulations: the difference between the mean particle settling velocity $\langle V_z \rangle$ and the terminal velocity V_T.

numbers to analyse the dynamics of inertial particles subject to gravity. This is a necessary first step to scrutinise such flows as potential structural models of subfilter turbulence for LES of particle-laden simulations of more complex flows. It has been observed that particle trajectories are non-trivially modified by the flow structures. More important, the mean particle settling velocity is different from that in the quiescent fluid. In some St parameter range, the settling velocity is enhanced due to preferential sampling of particle trajectories in the vortical flow field.

Acknowledgements The work has been supported by the National Science Centre (NCN, Poland) through the research project 2011/03/B/ST8/05677.

Received in 10 February 2017

References

[1] Drobniak S.: *Turbulence, from stochastic to deterministic approach*, Trans. Inst. Fluid Flow Mach. **110**(2002), 103–114.

[2] Fung J.C., Hunt J.C., Malik N.A., Perkins R.J.: *Kinematic simulations of homogenous turbulence by unsteady random Fourier modes*. J. Fluid Mech. **236**(1992), 281–318.

[3] Fung J.C.H., Perkins R.J.: *Particle trajectories in turbulent flow generated by true-varying random Fourier modes. Advances in Turbulence 2*, (H.-H.Fernholtz and H.E. Fiedler, Eds.), Springer 1989, 322–328.

[4] Khan M.A.I., Luo X.Y., Nicolleau F.C.G.A., Tucker P.G., Lo Iacono G.: *Effects of LES sub-grid flow structure on particle deposition in a plane channel with a ribbed wall.* Int. J. Numer. Meth. Biomed. Engng. **26**(2010), 999–1015.

[5] Knorps M., Pozorski J.: *An inhomogeneous stochastic subgrid scale model for particle dispersion in Large-Eddy Simulation.* [In:] *Direct and Large-Eddy Simulation* (J. Fröhlich, H. Kuerten, B.J. Geurts, V. Armenio, Eds.) Springer 2015, **IX**, 671–678.

[6] Marchioli C.: *Physics and modelling of particle deposition and resuspension in wall-bounded turbulence.* [In:] Particles in Wall-Bounded Turbulent Flows, (Minier J.P., Pozorski J., Eds.), Springer 2017, 151–208.

[7] Maxey M.R.: *The gravitational settling of aerosol particles in homogeneous turbulence and random flow fields.* J. Fluid Mech. **174**(1987), 441–465.

[8] Maxey M.R., Corrsin S.: *Gravitational settling of aerosol particles in randomly oriented cellular flow fields.* J. Atmos. Sci. **43**(1986), 1112–1134.

[9] Monchaux R., Bourgoin M., Cartellier A.: *Preferential concentration of heavy particles: A Voronoi analysis.* Phys. Fluids **22**(2010), art. 103304.

[10] Monchaux R., Bourgoin M., Cartellier A.: *Analyzing preferential concentration and clustering of inertial particles in turbulence.* Int. J. Multiphase Flow **40**(2012), 1–18.

[11] Pope S.B.: *Turbulent Flows.* Cambridge Univ. Press 2000.

[12] Pozorski J.: *Models of turbulent particle dispersion.* In: Mathematical Methods in Applications (A. Bartłomiejczyk, Ed.), Centrum Zastosowań Matematyki, Politechnika Gdańska 2015, Vol. 3, 247–262. (in Polish).

[13] Pozorski J., Apte S.V.: *Filtered particle tracking in isotropic turbulence and stochastic modelling of subgrid-scale dispersion.* Int. J. Multiphase Flow **40**(2009), 118–128.

[14] Pozorski J., Knorps M.: *Towards stochastic modelling of inertial particle dispersion in wall-bounded turbulent flows.* 9th Int. Conf. on Multiphase Flow, Firenze, Italy, 22-27 May 2016, Proc. on USB-pendrive, art. 969.

[15] Puzyrewski R., Pozorski J., Kleitz A., Laali A.R.: *Comparison of droplets separation ability of cascades operating with wet steam.* [In:] IX International Conference Steam Turbines of Large Output, Karlovy Vary 1989.

[16] Puzyrewski R., Sawicki J.: *Fundamentals of Fluid Mechanics and Hydraulics.* 3rd Edition, PWN Warszawa 2015 (in Polish).

[17] Rosa B., Pozorski J.: *Analysis of subfilter effects on inertial particles in forced isotropic turbulence.* 9th Int. Conf. on Multiphase Flow, Firenze, Italy, 22-27 May 2016, Proc. on USB-pendrive, art. 974.

[18] Voßkuhle M., Pumir A., Lévêque E., Wilkinson M.: *Collision rate for suspensions at large Stokes numbers – comparing Navier-Stokes and synthetic turbulence.* J. Turb. **16**(2014), 15–25.

[19] Wang L.P., Maxey M.R.: *Settling velocity and concentration distribution of heavy particles in homogeneous isotropic turbulence.* J. Fluid Mech. **256**(1993), 27–68.